

**Microstructure and Hardness Investigation of Different Welding
Passes in Weld Zones**

by

Muhammad Syazwan Azrie bin Yahaya
(13260)

Project Dissertation submitted in partial fulfilment of
the requirements for the
Bachelor of Mechanical (Hons)
(Mechanical Engineering)
SEPTEMBER 2013

Universiti Teknologi PETRONAS
Bandar Sri Iskandar
31750 Tronoh
Perak Darul Ridzuan

CERTIFICATION OF APPROVAL

Microstructure and Hardness Investigation of Different Welding Passes in Weld Zones

by

Muhammad Syazwan Azrie bin Yahaya

A project dissertation submitted in partial fulfilment of
the requirements for the
Bachelor of Engineering (Hons)
Mechanical Engineering

SEPTEMBER 2013

Approved by,

(Dr Mokhtar Awang)

Universiti Teknologi PETRONAS

Bandar Seri Iskandar

31750 Tronoh

Perak Darul Ridzuan

CERTIFICATION OF ORIGINALITY

This is to certify that I am responsible for the work submitted in this project, that the original work is my own except as specified in the references and acknowledgements, and the original work contained herein have not been undertaken or done by unspecified sources or persons.

(MUHAMMAD SYAZWAN AZRIE BIN YAHAYA)

ABSTRACT

Friction Stir Welding (FSW) is a solid state process for joining aluminium and other metallic alloys where the metal is not melted during the welding process. It was invented to substitute conventional welding of aluminium alloy. This report will covers the theoretical background of friction stir welding, literature reviews on related research works, implemented methodology, results and discussions and lastly conclusion. The objective of this study is to analyze the microstructure of different welding passes in weld zones as well as the hardness of the weld zones. Besides, it also will cover the systematic procedure for optical microscopy analysis for Al 6061-T6. The project will focus on three types of passes which is Pass A (single pass), B (double passes same side) and C (double passes different side). The welding tools were fabricated using CNC Machine and undergo heat treatment for hardening. Two plates of aluminium alloy work piece with similar dimension were set-up in butt joint configuration and clamped rigidly during welding operation. The work pieces were weld using different type of passes but the parameters will be similar for all passes. Welded workpieces that have been welded by the designed tools will be undergoing lab testing which are microstructure test and hardness test in order to rectify the difference of the weld results. The visual inspection on the weld joint show that double passes FSW experienced smaller worm hole defect than single pass. Microstructure investigation only shows slight different in size of grain boundary between all passes. The quantity of precipitates is highest at the TMAZ region compared with other regions. The double passes FSW same side (Pass B) exhibits highest hardness value with 61.1 HV in stir zone (SZ) compared with other two pass. However, all regions exhibit lower hardness value compared with parent material (PM) in all passes.

ACKNOWLEDGEMENT

Assalamualaikum w.b.t and Alhamdulillah,

Praise and thanks to Allah, this dissertation was finally completed and finished my Final Year Project. Highest appreciation goes to Dr. Mokhtar Awang, my supervisor, for his relentless patience and guidance throughout the project.

Also a special express gratitude for Mechanical Engineering Department of Universiti Teknologi PETRONAS for providing excellent support in terms of providing cutting edge knowledge and information along five years spent undergoing every single bit of valuable knowledge on Mechanical Engineering. My appreciation and gratitude also goes to the technical staff from Mechanical Engineering Department who are involved with this project, Mr. Shaiful, Mr. Jani Alang Ahmad, Mr. Adam, Mr. Zamil, Mr. Daniel and Mr. Kamarul for their enormous efforts on assisting me with the technical support and guidance towards this project.

Last but not least, thanks to my beloved family that always gives me full support for me in every condition and everyone who had been involved directly or indirectly in making and delivering this project succeed.

MUHAMMAD SYAZWAN AZRIE BIN YAHAYA

TABLE OF CONTENT

| | |
|--|-----------|
| CHAPTER 1 : INTRODUCTION..... | 1 |
| 1.1 Background Study | 1 |
| 1.2 Problem Statement..... | 4 |
| 1.3 Objective | 4 |
| 1.4 Scope of Study..... | 5 |
| CHAPTER 2 : LITERATURE REVIEW | 6 |
| CHAPTER 3 : METHODOLOGY..... | 11 |
| 3.1 Overall Project Methodology | 11 |
| 3.2 Identify the problem, objective and concept of project | 30 |
| 3.3 Fabrication of Welding Tool..... | 12 |
| 3.4 Welding Process | 15 |
| 3.5 Microstructure Investigation in Weld Zone | 13 |
| 3.6 Hardness Test | 28 |
| 3.7 Project Gantt Chart | 30 |
| 3.8 Key Milestone | 32 |
| CHAPTER 4 : RESULTS AND DISCUSSIONS | 33 |
| 4.1 FSW on Three Different Passes | 33 |
| 4.2 Microstructure Analysis..... | 36 |
| 4.3 Vickers Hardness Testing | 42 |
| CHAPTER 5 : CONCLUSIONS AND RECOMMENDATIONS | 45 |
| 5.1 Conclusion | 45 |
| 5.2 Recommendations | 46 |
| REFERENCES | 47 |
| APPENDIX | 50 |

LIST OF FIGURES

| | |
|---|----|
| Figure 1. 1: Schematic diagram of FSW process. ^[9] | 2 |
| Figure 1. 2: The existing zone after FSW process..... | 3 |
| Figure 2. 1: Schematic representation of overlapping weld passes in 5083-O aluminium alloy ^[16] | 6 |
| Figure 2. 2: Schematic representation of overlapping weld passes in 6063-T6 aluminium alloy ^[16] | 6 |
| Figure 2. 3 : Typical grain nugget appearance (Brown et. al)..... | 7 |
| Figure 2. 4 : Schematic diagram of SPW and DPW. (Xu et. el) | 8 |
| Figure 2. 5 : Microstructure of parent metal (a,b) and stir zone (c,d) of AA2024 ^[21] | 9 |
| Figure 3. 1: Overall project flow in FYP 1 and FYP 2..... | 11 |
| Figure 3. 2 : Bridgeport machine that was used for fabrication process..... | 13 |
| Figure 3. 3: Tool steel H13 is placed inside the furnace with heating element on both sides..... | 14 |
| Figure 3. 4: Flow of tool steel H13 hardening process. | 14 |
| Figure 3. 5: Condition of tool steel H13 after preheat, austenitize and air quench | 15 |
| Figure 3. 6: Aluminium workpiece is clamped into the jig..... | 16 |
| Figure 3. 7: The position of material and welding tool before welding started | 17 |
| Figure 3. 8: Pass A..... | 18 |
| Figure 3. 9: Pass B | 19 |
| Figure 3. 10: The workpiece is been weld by the welding tool..... | 19 |
| Figure 3. 11: Pass C | 20 |
| Figure 3. 12: Hand grinder is used to remove flash..... | 20 |
| Figure 3. 13: Aluminium welded plate is sectioned by using EDM machine..... | 21 |
| Figure 3. 14: Abrasive cutter is used to section small workpiece. | 22 |
| Figure 3. 15: Auto Mounting Press machine..... | 23 |
| Figure 3. 16: Workpiece that had been sample mounted. | 23 |
| Figure 3. 17: MetaServ 2000 Grinder machine. | 24 |
| Figure 3. 18: Comparison of sample before and after grinding | 25 |
| Figure 3. 19: Diamond particle used during polishing process..... | 26 |

| | |
|---|----|
| Figure 3. 20 : Optical Microscope | 28 |
| Figure 3. 21: Vickers Hardness test [30]..... | 29 |
| Figure 4. 1: FSW on Pass A | 33 |
| Figure 4. 2: Worm tunnel defect in Pass A. | 34 |
| Figure 4. 3: The presence of spiral chip and flash on Pass B welded plate. | 34 |
| Figure 4. 4: Presence of worm hole defects in Pass B | 35 |
| Figure 4. 5: Welded plate of Pass C..... | 35 |
| Figure 4. 6: Worm tunnel in Pass C welded plate. | 36 |
| Figure 4. 7: Grain boundary microstructure 100x of three main regions of Pass A (Keller’s etchant). | 37 |
| Figure 4. 8: Grain boundary microstructure 100x of three main regions of Pass B (Keller’s etchant). | 38 |
| Figure 4. 9: Grain boundary microstructure 100x of three main regions of Pass C (Keller’s etchant). | 39 |
| Figure 4. 10: Two different parent metal microstructure with 100x magnification (Keller’s etchant) | 41 |
| Figure 4. 11: Schematic diagram of Vicker’s micro-hardness..... | 42 |
| Figure 4. 12: Vickers hardness (HV) across the welded plate | 43 |

LIST OF TABLES

| | |
|--|----|
| Table 3. 1: Welding parameters for trial run FSW | 16 |
| Table 3. 2: Welding parameters for FSW on three different passes. | 17 |
| Table 3. 3: Parameters for sample mounting..... | 23 |
| Table 3. 4: Procedure for grinding process | 24 |
| Table 3. 5: Procedures for polishing. | 25 |
| Table 3. 6: Details of Keller’s Reagent..... | 27 |
| Table 3. 7 : Gantt chart for FYP 1 | 30 |
| Table 3. 8: Gantt chart for FYP 2 | 31 |
| Table 3. 9: Key milestones..... | 32 |
| Table 4. 1: HV value of nine indentation hardness points..... | 42 |

CHAPTER 1

INTRODUCTION

1.1 Background Study

Friction Stir Welding (FSW) is a solid-state joining or welding method that was developed by The Welding Institute (TWI) in early 90s [1]. FSW involves a non-consumable and rotating tool to weld the work pieces together by stirring together the surrounding material. It was initially developed for use on aluminium alloys because of the lower temperatures and stresses required to weld those alloys and the ready availability of tool materials to perform the welding [2]. Compared with the usual welding techniques, FSW is good energy consumption, environment friendly and more reliable welding process [3].

There are two main components in FSW which is the cylindrical-shouldered tool and small diameter pin. The welding tool is driven into the weld seam between workpiece that are firmly clamped to an anvil and traversed across the length of the seam to form a solid joint [4, 5]. The rotating pin that was inserted into the material will create the heat around the rotating part thus allowing the material to be softened and highly deformed ($\epsilon > 40$) [6]. The pin will penetrates the intended seam to the entire depth of the pin which is usually 80% or 90% of the workpiece thickness. Further insertion [7] of the tool will cause the shoulder part to be intact with the workpiece. This will indirectly produce the frictional force that will increase the generation of heat around the pin and causing the material to be softened and stirred. Besides that, high hydrostatic pressure needs to be maintained by the load on the tool shoulder.

During FSW, as the pin is moved in the direction of welding, the leading face of the pin by the assist of special pin profile, forces the plasticized material to the back of the pin while applying a significant amount of forging force to join the weld metal. The welding of the material is facilitated by critical plastic deformation in the solid state which involves dynamic recrystallization of the base material [8]. The different in plastic

flow characteristics causes the different microstructures to form in both sides of the workpiece. The advancing and retreating side orientation during FSW can be known from the tool rotation and the longitudinal direction of the weld. As seen in Figure 1, FSW tool which is on the bottom side of the workpiece if seen from the plan view is rotating in the counter-clockwise direction and travel to the up side of the workpiece. Thus, the right side of the workpiece is counted as advancing side because the tool rotation direction is the same as the tool travel direction which is horizontal to the top side whereby the retreating side is on the left where the tool rotation direction opposes the direction of the tool travel direction [9].

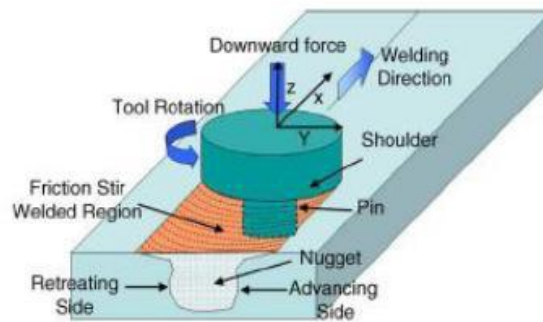


Figure 1. 1: Schematic diagram of FSW process. [9]

Despite the material used in FSW, there are four microstructure zones that result from the welding process. The area of all four zones comprises as the Stir Zone (SZ), Thermo Mechanically Affected Zone (TMAZ), Heat Affected Zone (HAZ) and parent material (PM). In SZ, the main element is known as the weld nugget, which lies at the center of the weld along the weld seam, where the heat accumulation and deformation are the greatest. This zone is surrounded by the remaining two constituent zones, which is TMAZ that surrounds the SZ and HAZ that surrounds the outside part of the TMAZ [9]. The formation of above regions is affected by the material flow behaviour under the action of rotating non-consumable tool [10] which is predominantly influenced by the number of passes that are used and also process parameters [11] during FSW. However, the available literature focussing on the effect of passes on the microstructure in FSW is very minimal. Hence, in this investigation, an attempt has been made to understand the effect of different welding passes on grain boundary and weld zones.

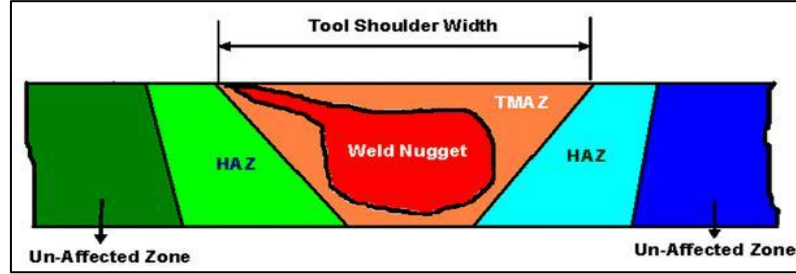


Figure 1. 2 : The existing zone after FSW process

A number of potential advantages of FSW processes have been identified. They are excellent mechanical properties in the joint area, solid-phase process fine recrystallized microstructure, no loss of alloying elements low production cost, low environmental impact, minimal surface cleaning required, decreased fuel consumption in lightweight aircraft, automotive and ship applications, easily automated on simple milling machines and can operate in all positions (horizontal, vertical, etc).

However, some disadvantages of the process have been identified. One of them is the single pass welding speeds in some sheet alloys are slower than for some mechanised arc welding techniques [12]. Other disadvantages in FSW process are large down forces needed with heavy-duty clamping necessary to hold the plates together and exit hole left when tool is withdrawn. Besides, it is less flexible than manual and arc processes (difficulties with thickness variations and non-linear welds).

FSW process is used particularly for welding aluminium alloys in marine industries, aerospace, automotive and rail industry [13]. Nowadays, the process is being moved into fabrication of complex assemblies, yielding significant quality and cost improvements. As the process is maturing, designers are taking advantage of the process, by designing the product specifically for the FSW process.

1.2 Problem Statement

FSW can be considered as a very unique process that solves the difficulties that occur in some of the welding process. Many researches regarding FSW have been performed but only a small amount of research has been done specifically about the effect of pass in FSW. Number and flow of the passes play important role in ensure the workpiece soften and deform in a perfect way. Different passes also will affect the microstructure of the weld material as well as the grain boundary on the welded zone and this will affect in the weld quality. For example, the fabrication of aeroplane using friction stir welding needs very high quality of welded metal. Thus, the impact of different welding passes of FSW in term of quality is unknown and will be investigate in this research.

1.3 Objective

There are three main objectives in this project:

- To evaluate the microstructure of three different welding passes those undergo FSW.
- To establish a systematic procedure for optical microscopy analysis for Al 6061-T6 friction stir welded plates.
- To access the hardness of double passes FSW welded plates.

1.4 Scope of Study

For this project, the study will focus on welding process which is friction stir welding (FSW). FSW will be use to weld and join the aluminium alloy in different number of passes. CATIA software will be used in this project in designing the FSW welding tool. The welding tool's pin used will be tapered shape. In fabrication scope, CNC milling machine will be used while for hardening process, furnace will be used for the heat treatment. For material scope in this research, similar material will be used which is Aluminium 6061-T6 with equal thickness of 10mm. Lastly, this study also will focus on the microstructure in all three passes that will be seen by using optical microscope (OM). The microstructure then will be examined in order to get their individual characteristics.

CHAPTER 2

LITERATURE REVIEW

Many studies have been done on FSW such as the study of the welding tool geometry [14], metal flow during FSW of 7075-T651 aluminium alloy [15], microstructure, crystallographic texture of mechanical properties of AA2017A and many more. However, only a minimal amount of researches has been performed regarding the effect of passes during FSW towards the microstructure in the weld zones. One of them is the study of the effect of overlapping friction stir welding passes in the quality of welds [16]. In the study, Leal *et. al* performed four overlapping passes with AA5083-O and three overlapping passes with AA6063-T6. The process parameters used on the initial pass were maintained for all passes. However, the travel speed and rotation speed applied on AA5083-O is slightly lower than AA6063-T6.

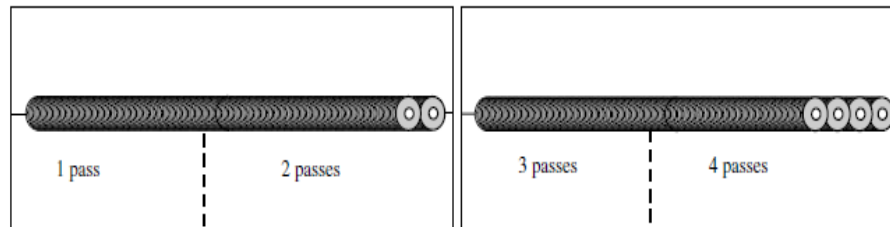


Figure 2. 1: Schematic representation of overlapping weld passes in 5083-O aluminium alloy ^[16]

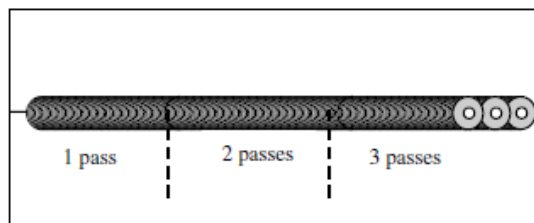


Figure 2. 2 : Schematic representation of overlapping weld passes in 6063-T6 aluminium alloy [16]

As a result, the execution of successive overlapping passes does not substantially change the grain size in the stir zone which is between 5 to 10 μm and there is also no substantial change in mechanical properties. In the weld done by overlapping passes, the

microstructure in the different regions of the weld is identical as observed in single pass weld. However, the passes flow in the research is only using one direction and not using the backward flow.

In other study, Brown *et. al* [17] had performed multi-pass friction stir welding in alloy 7050-T7451. The plates were square-butt welds and five overlapping passes had been done. For the result, the weld cross-section in the single pass is almost similar with the cross-section of the five overlapping passes. The grain sizes in the nugget zone for all overlapping passes only show a slight variation, which was consistent with the similar measured pin temperatures. The grain size of nugget is essentially unchanged by application of multiple weld passes. In previous studies [18, 19] it has been observed that the welding temperature is closely related to the final grain size in the weld nugget regardless the number of passes performed in the FSW process.

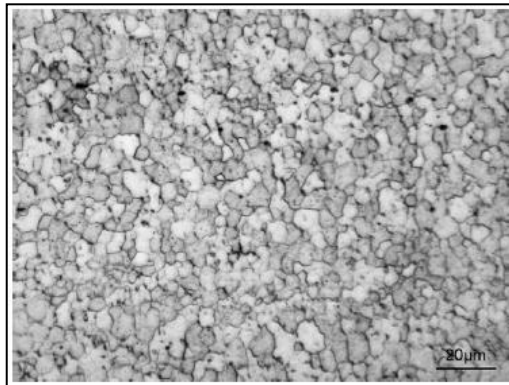


Figure 2. 3 : Typical grain nugget appearance (Brown *et. al*)

The application of friction stir single pass welded (SPW) and double pass welded (DPW) had been used in several research. For example, Xu *et. al* [20] had tested SPW and DPW lap joints in order to understand the microstructure and fatigue properties of friction stir lap welds in aluminium alloy AA6061-T6. In the research, the DPW process was used in order to evaluate whether the second pass weld can improve the weld quality. However, the microstructure was different as it used lap weld joint instead of butt-weld joint which will be use in this research.

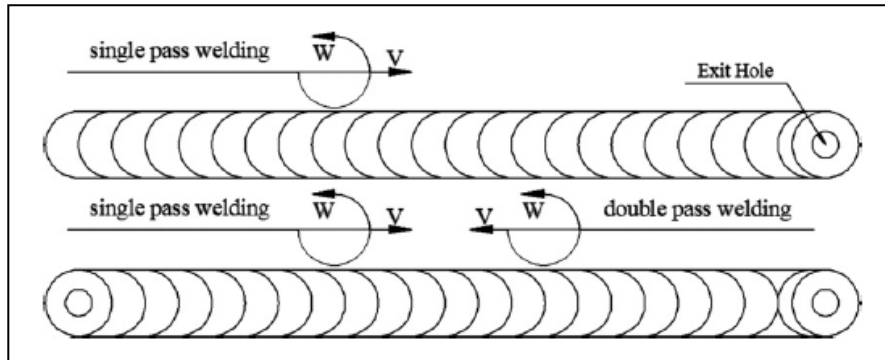


Figure 2. 4 : Schematic diagram of SPW and DPW. (Xu et. el)

In other hand, Koizumi [26] and his colleagues had performed a research regarding two pass friction stir welding of magnesium alloy. In their research, the welding passes were done on the upper and lower surface of the material. However, they also did not use the backward flow and only used the same direction for both surfaces. Using same direction for both surfaces will disturb the advancing and retreating side of the workpiece. They claimed that the grain size of two passes is smaller than one pass. However, that was the effect of the smaller tool as they used larger tool for single pass and smaller tool for the double passes. They also claimed that the hardness of two or double passes was higher than one pass FSW.

Next research of FSW which was done by Armagan *et. al* [27] study about the effect of double passes on FSW of polyethylene. However in their research, they did not state the direction of the passes that they used. They claim that double passes of FSW can increase the joint mechanical properties as well as eliminate the defects that appear in the first pass. This result is similar to the research done by Christian [28] and his colleagues which claimed that several passes of FSW can repair the defects done by the single pass.

Despite the material used in FSW, the research of microstructure in FSW has always been performed. Mohammadtaheri *et. al* [21] had performed the research regarding the final microstructure of 2024 aluminium alloy. In the research, the microstructure of the parent material and stir zone was studied. The grain in the parent material was slightly elongated and larger than the grain in stir zone which had been recrystallized during the FSW process.

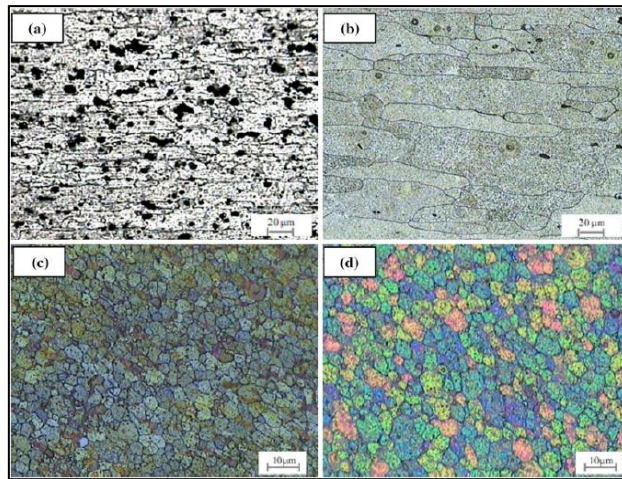


Figure 2. 5 : Microstructure of parent metal (a,b) and stir zone (c,d) of AA2024 ^[21]

Fonda *et. al* [22] in the research of the microstructural evolution in HAZ stated that at the center of the weld, the nugget displays characteristic concentric rings in its interior and a well-defined outer edge on the advancing side. It showed that the weld nugget in stir zone consist of a fine and equiaxed grains. The refined microstructure is referred to the dynamic recrystallization incident that takes place in its area at elevated temperature. ^[21] High temperature from the greater stirring will result in larger grains from the growth of recrystallized grains but low stirring of weld metal will results in less dynamic recrystallization and larger grain.

On the other hand, in producing a defect free weld with good microstructure, Frigaard *et. al* [23] suggests that maintaining the tool rotational speed and position of the tool head in x, y and z axes are very important. Besides, traverse speed and downward force are also critical part in FSW. As the weld zones behaviour is affected by the tool geometry, the design of the tool shoulder and pin is a critical factor as a good tool can improve both the quality of the weld. Reynolds *et. al* [24] had tested several different variations of cylindrical pins with a concave shoulder to show that defect-free friction stir welds in 8.1mm thick 2195 aluminium alloys could be produced with pin diameter ratios ranging from 2 to 1 to 3.125 to 1. Besides, the material flow during FSW will increase if the pin with a triangular tool pin is used rather than the cylindrical pin [25]. Features such

as thread and flutes on the pin are understood can gain the heat generation rate due to larger interfacial surface area thus improving the material flow during FSW. It is also desirable that the tool material is sufficiently strong, tough and hard wearing, at the welding temperature. Furthermore, it should have a good oxidation resistance and a low thermal conductivity to minimize heat loss and thermal damage.

CHAPTER 3

METHODOLOGY

3.1 Overall Project Methodology

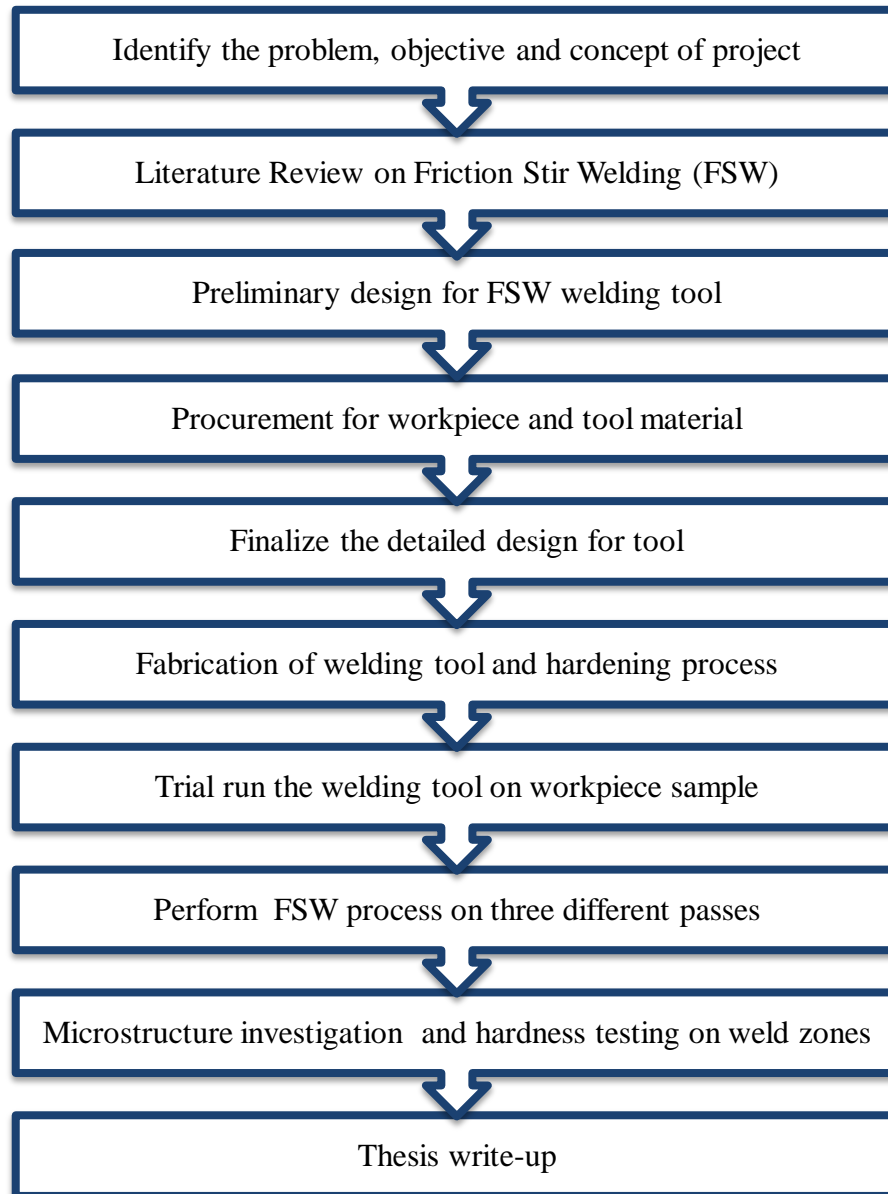


Figure 3. 1: Overall project flow in FYP 1 and FYP 2

3.2 Identify the problem, objective and concept of project

Firstly, the problem, objective and concept of this research need to be identify first. Basicaly, this research will focuses on different welding process in FSW and do the microstructure and hardness investigation. From the researches, the author decides to use Aluminium 6061-T6 with 100mm x 100mm x10mm dimension as material for workpiece and 25mm diameter tool steel H13 as welding tool material.

3.3 Fabrication of FSW Welding Tool

The fabrication of welding tool is one of the important processes of FSW. This is because the design and material of welding tool can affect the quality of the welding. The welding tool must be strong and low resistant to wear at high welding temperature. Besides, it also must have low thermal conductivity in order to reduce the heat loss and thermal damage to the machinery.

3.3.1 Design of welding tool using CATIA

The welding tool is designed using CATIA VR12 software. The main reason for the tool design is to ease the fabrication of the tool later. The preliminary design has been revised by supervisor and lab technician in order to fabricate the tool with proper dimension. For the tool design, the author has decided to design the tool with taper-shaped pin of 5mm diameter with 8mm height and 25mm shoulder diameter. The taper-shaped pin is chosen because it can reduce the defects that form during the welding process.

3.3.2 Fabrication using Bridgeport Machine

Fabrication of welding tool which is tool steel H13 was done on 1st August 2013. This process had been done by following the final design sketch that the author had done. Bridgeport Romi Powerpath 15 machine had been used in completing the fabrication of the welding tool. The machine is controlled electronically via a computer menu style interface where the program is customized and displayed at the machine, along with a simulated view of the process. The operator of the machine needs a high level of

expertise to carry out the process. However the knowledge base is broader compared to the older production machines where intimate knowledge of each machine was considered essential. The process only takes about 15 minutes to setup the program code into the machine and 10 minutes to fabricate the tool.



Figure 3. 2 : Bridgeport machine that was used for fabrication process

3.3.3 Hardening Process of Welding Tool

Hardening process or heat treatment of tool steel H13 was done on 8th August 2013. The process was done by using Carbolyte HTF 18/15 furnace. The purpose of heat treatment process is to control the heating and cooling of metals in order to alter their physical and mechanical properties without changing the product shape. Before the hardening process was done, the author had done some research regarding the method and parameter needed in the heat treatment or hardening process. There are several phases in hardening process which are pre heating, austenitizing (high heat) and lastly quenching phase. During the pre heating, tool steel H13 was preheat at 750°C for two hours. Then, the temperature was raised to 1010 °C in the austenitizing phase and dwell for one hour. The main purpose of austenitizing is to dissolve the carbides to the matrix that acquires an alloying content that gives the hardening effect without becoming coarse-grained and brittle. This is very important as the welding tool cannot be brittle as the welding process may break the tool.



Figure 3. 3: Tool steel H13 is placed inside the furnace with heating element on both sides

In austenitizing phase, a transformation occurs from ferrite to austenite [29]. The tool steel H13 is then air quenched until it was cool to the room temperature. The author used air quenched instead of oil quenched as the oil quenched will make tool steel brittle. During the quenching phase, the carbon atoms do not have time to reposition themselves and they are fixed in position which results in high microstresses. This will result in increasing of hardness. This structure is called as martensite. However, untransformed austenite, called as retained austenite is also present in the quenched structure. The microstructure of tool steel after quenching phase contains carbides, martensite and also retained austenite. The general flow of hardening process is illustrated in figure below:

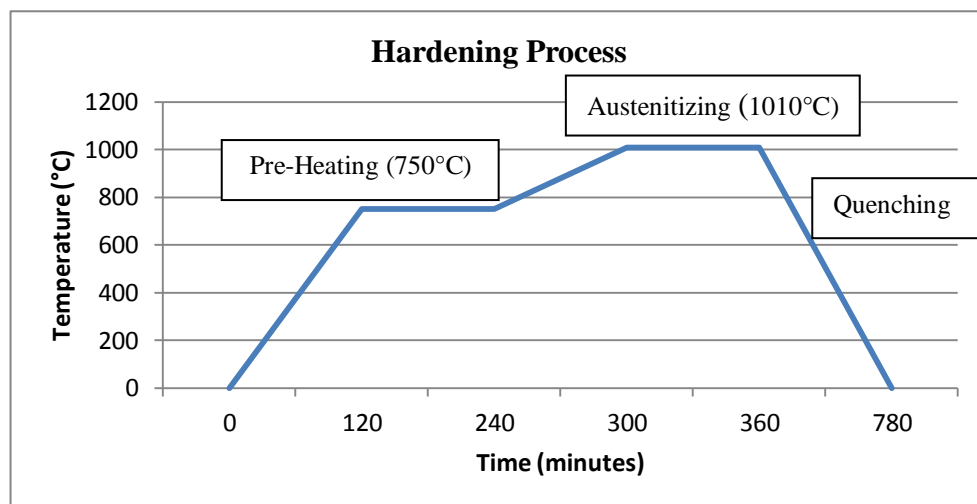


Figure 3. 4: Flow of tool steel H13 hardening process.



Figure 3. 5: Condition of tool steel H13 after preheat, austenitize and air quench

3.4 Welding Process

After the hardening process, the welding tool will be clamp by the clamber inside the Bridgeport VMC 2216 XV machine in order to run onto the workpiece later. However, as the maximum workpiece size that the clamber can hold is 20mm, half of the welding tool material is lathed is reduced for 5mm in order to enable tight clamping of the clamping. This is very important to make sure that the welding tool is not wobbling during the welding process. The Bridgeport machine is controlled using customized control that has the ability to move the spindle vertically along the X, Y and Z-axis. This extra degree of freedom permits their use in many applications such as die sinking and engraving applications.

Before the welding start, the aluminium workpiece need to be clamped by the jig. Jig plays important role in order to give support to the workpiece as well as give a better platform during the welding process. Jig will hold the workpiece firmly to make sure that there is no movement of the workpiece during the welding that can be dangerous if the workpiece is bounced away.

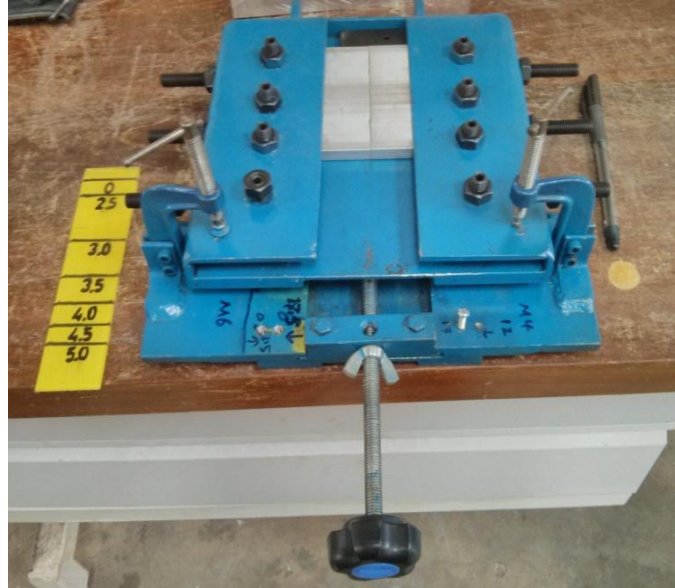


Figure 3. 6: Aluminium workpiece is clamped into the jig

3.4.1 Trial run on workpiece sample

The FSW trial run is done to test the welding tool that already been fabricated and also the result of the welding. By doing test, the suitable condition and parameters such as the rotation speed and traverse speed during the welding can be emphasize in the real process. The trial was only been done four times using different parameters.

Table 3. 1: Welding parameters for trial run FSW

| Run | Feed Rate (mm/min) | Tilt Angle (°) | Rotational speed (rev/min) | Depth of penetration (mm) | Dwell time (s) | Length of weld line (mm) |
|-----|--------------------|----------------|----------------------------|---------------------------|----------------|--------------------------|
| #1 | 20 | 2 | 1000 | 8 | 25 | 70 |
| #2 | 30 | 3 | 1200 | 8 | 30 | 70 |
| #3 | 20 | 2 | 1500 | 8 | 35 | 70 |
| #4 | 30 | 3 | 1800 | 8 | 40 | 70 |

3.4.2 FSW on three different passes

Before conducting FSW on three different passes which are Pass A, Pass B and Pass C, there are several parameters that need to be maintain throughout all passes. The welding parameters that have been chosen are:

Table 3. 2: Welding parameters for FSW on three different passes.

| No | Parameters | Details |
|----|-------------------------------|-----------|
| 1 | Tool rotational speed (rpm) | 1200 |
| 2 | Transverse speed (mm/m) | 30 |
| 3 | Tilting angle ($^{\circ}$) | 3 |
| 4 | Spindle direction | Clockwise |
| 5 | Plunging dwell time (s) | 20 |
| 6 | Withdrawn dwell time (s) | 4 |
| 7 | Depth of penetration (mm) | 8 |
| 8 | Weld line length (mm) | 70 |
| 9 | Advancing and retreating side | Maintain |

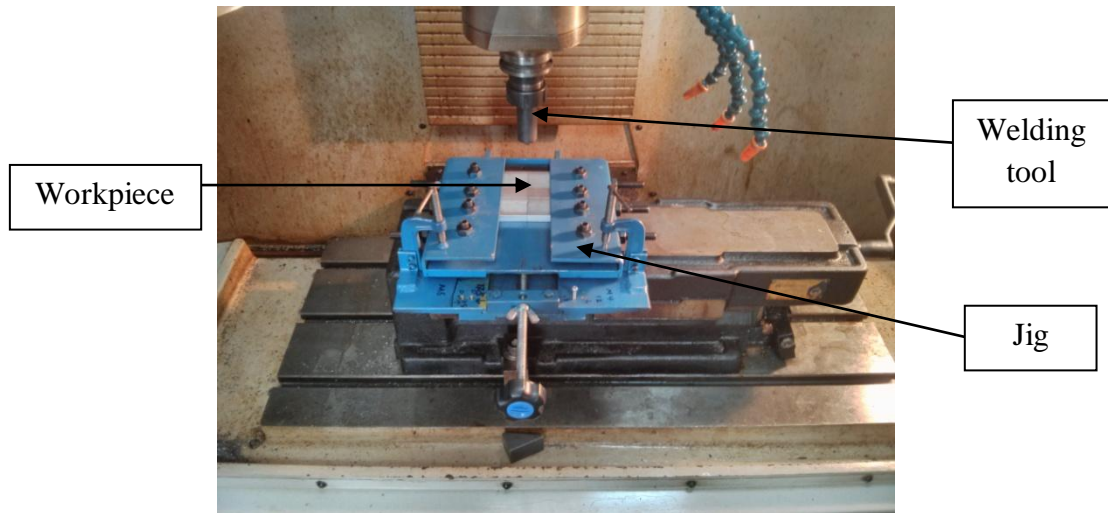


Figure 3. 7: The position of material and welding tool before welding started

The jig is placed inside the Bridgeport machine under the welding tool clamp. It is tightened and the workpiece is double checked to make sure it is already clamped tightly. Both of the aluminium plates need to be assembled close to each other and should not have any gap between each other. After the coding is keyed in, the welding starts at 25mm from the edge. The welding will go along the aluminium for 70mm before stopping. After the welding stops, coolant liquid is used to cool down the workpiece and also the jig. This is done to ease the opening of the workpiece. Before the workpiece is dragged out from the clamp, the allen key is used to loosen the bolt on the jig. After that, the next workpiece is welded using the same parameter with different passes.

Pass A (Single Pass)

For the first type of pass, the welding tool will rotate in a clockwise direction and move longitudinally forward from the start point to the end point (exit hole) of the workpiece. The right side of the workpiece will be the retreating side while the left side will be the advancing side. For Pass A, only single pass welding is used which is the upper part of the aluminium.

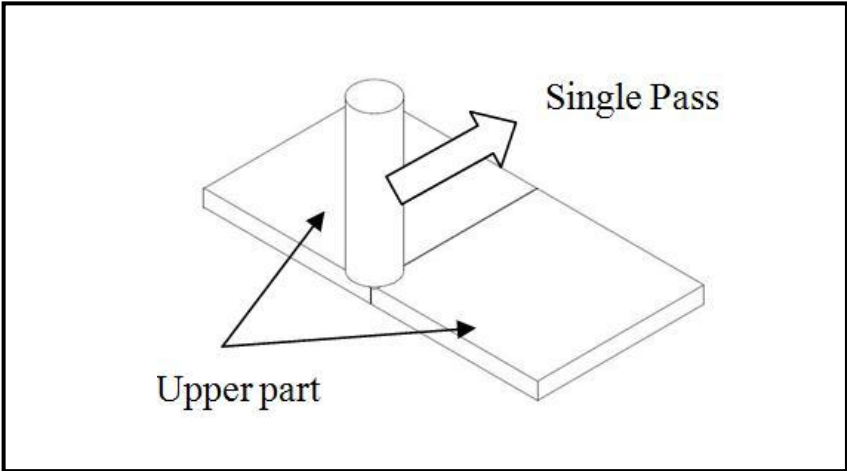


Figure 3. 8: Pass A

Pass B (Double Pass on Same Side)

For the second type of pass, the welding tool will rotate in a clockwise direction and move longitudinally forward from the starting point to the end point of the workpiece. Then, the welding tool will move longitudinally backward from the exit hole of the workpiece back to the starting point.

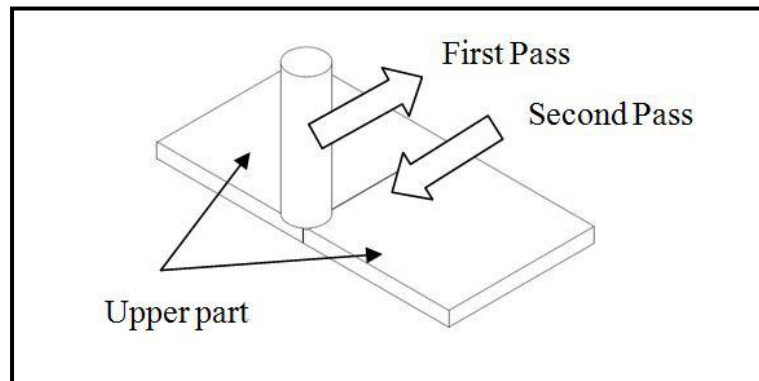


Figure 3. 9: Pass B

As for the forward pass the direction of the spindle is in the clockwise direction, the rotation spindle is changed to counter-clockwise direction in order to maintain the advancing and retreating side. This step is very important in order to keep the parameter constant for all three passes.



Figure 3. 10: The workpiece is been weld by the welding tool.

Pass C (Double Passes on Different Side)

For the final pass, it include two passes whereby the welding tool will move from starting point to the exit hole on the upper part of the workpiece and then moving backward from the exit hole to the starting point on the bottom part of the workpiece. Both of the passes are done using clockwise direction that will maintain advancing and retreating side.

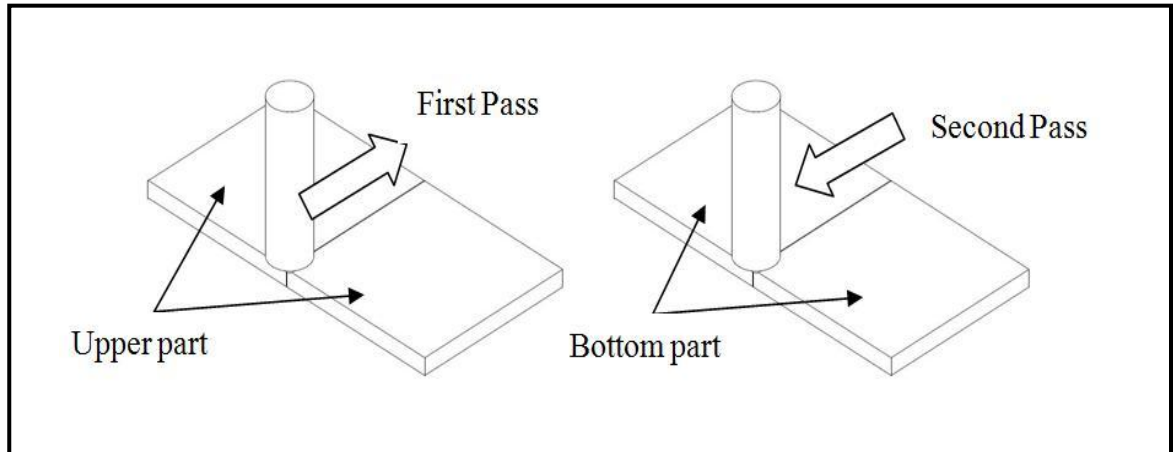


Figure 3. 11: Pass C

For Pass C, after the first pass is done, the workpiece need to be drag out of the jig before the second pass can be done. This is because during the welding for the first pass, the flash is splashed around the weld zone and the second pass which will be run on the bottom part cannot be done due to uneven surface. Thus, the flash needs to be remove using the hand grinder and then chisel is used to even the surface.



Figure 3. 12: Hand grinder is used to remove flash.

3.5 Microstructure Investigation on Weld Zones

All the microstructure of the weld zones of the different welding passes are examined using the optical microscope. The investigation will be done by focussing on the differences of microstructure between all the passes mainly on the stir zone, thermo-mechanically affected zone, heat affected zone and parent material regions. Before the microstructure can be reveal by using optical microscope (OM), all of the samples need to undergo metallography process or sample preparation that includes several steps which are sectioning, sample mounting, grinding, polishing and lastly, etching.

3.5.1 Sectioning

Sectioning is cutting or separating the work piece from a larger size to smaller size. Sectioning can be done by using non-ferrous abrasive cutter and also electrical discharge machine (EDM). In this project, both equipments are used. Sectioning is only been done on the intended area to be examined which are the welded area region and parent metal. Because of the large size of welded aluminium plate which is 100mm x 100mm x 10mm, EDM machine is firstly used to cut the welded plate into several small plates. Before using EDM, the sample is marked to make sure the lines that need to be cut are clear.

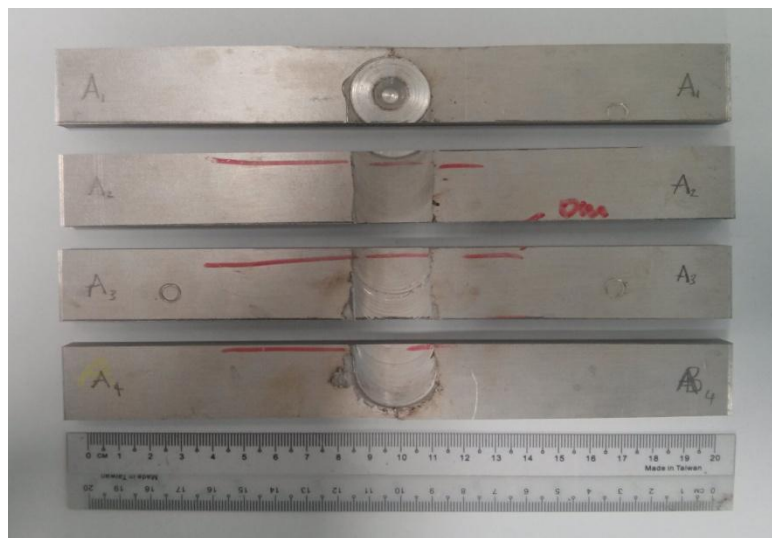


Figure 3. 13: Aluminium welded plate is sectioned by using EDM machine

After using EDM, abrasive cutter is used to section the plate smaller. Abrasive cutter is used for the finishing of the sectioning part as it only can tolerate small workpiece. The samples need to be section smaller as they need to be mounted later therefore the size of the sample should not be larger than the diameter of the mounting base which is about 27mm in diameter.



Figure 3. 14: Abrasive cutter is used to section small workpiece.

3.5.2 Sample Mounting

After the workpiece had been sectioned into small samples, they will be mounting. The main purpose for sample mounting is to give support and stable base for the sample. Besides, the mounted samples will be easier to grind and polish later as they can be easily hold and does not give much difficulty that the samples that do not mount. Sample mounting is done by using Auto Mounting Press. Cleansing agent is swabbed first on the base and then the phenolic powder is used to make the mount. The parameters used for sample mounting are tabulated below:

Table 3. 3: Parameters for sample mounting

| Parameter | Details |
|------------------|----------------|
| Heating time | 1.5 minutes |
| Cooling time | 5.0 minutes |
| Pressure applied | 3500 psi |

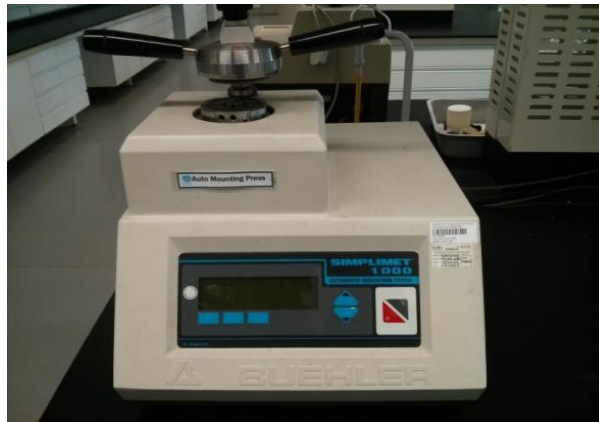


Figure 3. 15: Auto Mounting Press machine

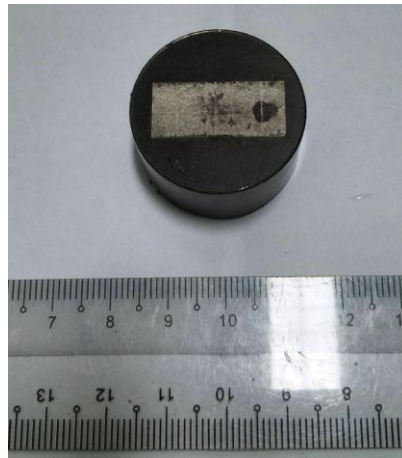


Figure 3. 16: Mounted sample.

3.5.3 Grinding

After the sample had been mounted, it will undergo grinding process. The aims of the grinding process are:

- To minimize thickness of damaged layer from to the sectioning process.
- To prepare a flat and even surface while introducing only some residual or superficial deformation that can be eliminated during polishing.

Grinding is typically done using rotating discs covered with silica-carbide (SiC) paper and using water as lubricant. During grinding, light pressure should be applied at the centre of the sample. Before proceeding to the next grinding steps, ensure the scratches from the current step are in a single orientation. Grinding is done until all the blemishes from previous steps have been removed. MetaServ 2000 Grinder Machine is used in this process. The steps for grinding the aluminium alloy sample are shown in the table below:

Table 3. 4: Procedure for grinding process

| Step | Abrasive | Gradation (grit) | Lubricant | Speed (rpm) |
|------|----------|------------------|-----------|-------------|
| 1 | SiC | 240 | H2O | 200 |
| 2 | SiC | 400 | H2O | 200 |
| 3 | SiC | 600 | H2O | 200 |
| 4 | SiC | 1200 | H2O | 200 |



Figure 3. 17: MetaServ 2000 Grinder machine.

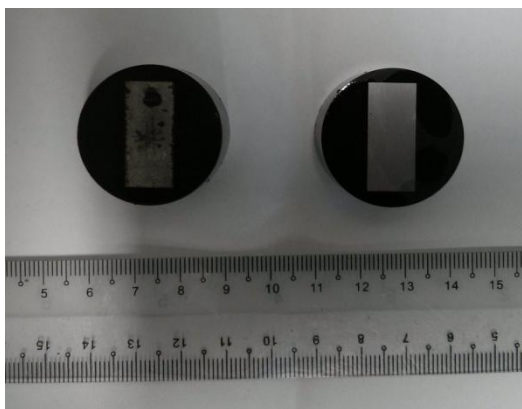


Figure 3. 18: Comparison of sample before and after grinding

3.5.4 Polishing

After the sample had been grind, it will undergo polishing process. The main purpose of polishing is to produce a scratch-free mirror like finish on the sample. This is because mirror like finish is needed to observe the true microstructure. Polishing is done by using MetaServ 2000 Polisher. It consist of rotating discs covered with soft cloth impregnated with micro-particles of diamond or other media. The procedures for polishing are shown in table below:

Table 3. 5: Procedures for polishing.

| Step | Cloth | Gradation (micron) | Polishing Paste | Speed (rpm) | Time (min) |
|------|---------|-----------------------|---------------------------|----------------|---------------|
| 1 | Napless | - | Diamond suspension liquid | 170 | 0.5 |
| 2 | Napless | 3 | Diamond particle paste | 170 | 1.0 |
| 3 | Napless | 1 | Diamond particle paste | 170 | 1.5 |



Figure 3. 19: Diamond particle used during polishing process

3.5.5 Etching

Etching process is the last process of the sample preparation. A polished sample is etched either by swabbing a cotton tip dipped in etchant, by immersing or spraying the sample with the etchant. The objectives of etching process are:

- To attack and reveal the grain boundaries and the interface regions between the matrix and phase constituent.
- To remove final thin layer of deformation.
- To cover selected phase constituent surface with a thin film of chemical reaction products that improve or reveal contrast between different structure components.

Each etchant usually has different function and only apply to certain material only. For aluminium alloy, the recommended etchant used to reveal the grain boundary is Keller's Reagent. Details of the Keller's Reagent are tabulated below:

Table 3. 6: Details of Keller's Reagent

| Etchant Name | Composition | Procedure | Remarks |
|---------------------|--|--|---|
| Keller's Reagent | <ul style="list-style-type: none"> • 190mL Distilled water • 5mL Nitric acid • 3mL Hydrochloric acid • 2mL Hydrofluoric acid | <ol style="list-style-type: none"> 1. 3-4 minutes swabbing. 2. Rinse with water and ethanol. 3. Dry the specimen. | <ul style="list-style-type: none"> • For most aluminum and aluminum alloys. • Only use fresh etchant. |

Etching process needs to be done in stages, beginning with light attack and then proceed to examination in the microscope and lastly further etching if required. This is because an over-etched sample requires a repeat of the polishing procedure and time consuming.

3.5.6 Optical Microscopic

After the sample had completed the sample preparation, light - optical microscope (OM) is used to examine the microstructure under magnification. Contrasts in the image produced result from differences in reflectivity of the different regions of microstructure. Usually, course focus and fine focus knob are played around in order for microstructure to display. The main focuses in this process are to find the most clear microstructure which will be consist of advancing and retreating side, grain boundary, impurities and others.



Figure 3. 20 : Optical Microscope

3.6 Hardness Test

Hardness is a characteristic of a material that enables it to resist plastic deformation. To measure the hardness, hardness testing is done. For example, micro-hardness tests such as Vickers and Knoop are applicable when surface hardness or coating hardness is measured while macro-hardness tests such as Rockwell and Brinell are usually used to test for rapid routine hardness measurements. Principle of any hardness test method is usually forcing an indenter into the sample surface followed by measuring dimensions of the indentation. Hardness is not fundamental property and its value depends on the combination of yield strength, tensile strength and modulus of elasticity.

3.6.1 Vickers Hardness Test

In Vickers micro-hardness testing, the sample is indented using the diamond indenter which is right pyramid with a square base and an angle of 136 degrees between opposite faces subjected to a load of 1000 gf. The dwell time for the load is only applied for 10 seconds. After the removal of the load, the two diagonals of the indentation that left in the surface of the sample after are measured using a microscope. The Vickers hardness is the amount obtained by dividing the kgf load by the square mm area of indentation. The Vickers Hardness number is calculated by the formula:

$$HV = [2 F \sin 136/2] / d^2$$

where;

F = Load (kgf)

d = Arithmetic mean of the two diagonals, d1 and d2 (mm)

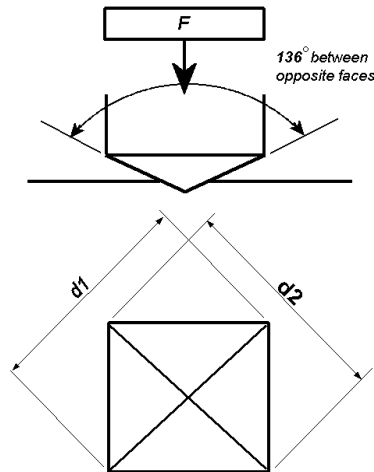


Figure 3. 21: Vickers Hardness test [30]

3.7 Project Gantt Chart

Table 3. 7 : Gantt chart for FYP 1

| Detail | W1 | W2 | W3 | W4 | W5 | W6 | W7 | W8 | W9 | W10 | W11 | W12 | W13 | W14 |
|---|----|----|----|----|----|----|----|----|----|-----|-----|-----|-----|-----|
| Literature review on FSW | ● | ● | ● | ● | | | | | | | | | | |
| Procurement of workpiece and tool material. | | | | | ● | ● | | | | | | | | |
| Designing the welding tool | | | | | | ● | ● | ● | | | | | | |
| Fabrication of welding tool (CNC) | | | | | | | | | ● | ● | | | | |
| Hardening process of welding tool | | | | | | | | | | | ● | | | |
| Trial run | | | | | | | | | | | | ● | ● | ● |

● indicates activities that had been done

Table 3. 8: Gantt chart for FYP 2

| Detail | W1 | W2 | W3 | W4 | W5 | W6 | W7 | W8 | W9 | W10 | W11 | W12 | W13 | W14 |
|---------------------------------------|----|----|----|----|----|----|----|----|----|-----|-----|-----|-----|-----|
| Literature review on FSW | ● | ● | ● | | | | | | | | | | | |
| Perform FSW on three different passes | | ● | ● | ● | ● | | | | | | | | | |
| Surface preparation | | | | ● | ● | ● | | | | | | | | |
| Microscopy analysis | | | | | | ● | ● | ● | ● | | | | | |
| Thesis write-up | | | | | | | | | | ● | ● | ● | ● | ● |

3.8 Key Milestone

Table 3. 9: Key-milestones

| No. | Milestones | Date |
|--------------|---------------------------------|---------------------------------|
| FYP 1 | Fabrication of welding tool | 3 th August 2013 |
| | Hardening process of tool | 10 th August 2013 |
| | Trial run | 23 rd August 2013 |
| FYP 2 | Perform FSW on different passes | 15 th September 2013 |
| | Surface preparation of specimen | 20 th October 2013 |
| | Microstructure Analysis | 10 th November 2013 |
| | Thesis Submission | 27 th December 2013 |

CHAPTER 4

RESULTS AND DISCUSSIONS

4.1 FSW on Three Different Passes

Friction stir welding had been done on three different welding passes which are Pass A, Pass B and Pass C. For this section, brief discussions are explained to see the different outcome by applying different sets of parameters in the welding procedure.

4.1.1 Pass A (Single Pass)

Pass A is the first friction stir welding runs on the Aluminium 6061-T6. Based on the figure of welded plate below, through visual examination, it can be observed that there is no worm tunnel at the exit hole which indicates that the material is stirred and mixed well at the end part of the welding. For the side, as the spindle rotates in a clockwise direction, the advancing side will be on the left side while the retreating side will be on the right side. In addition, the splash also occurs along the welding line.

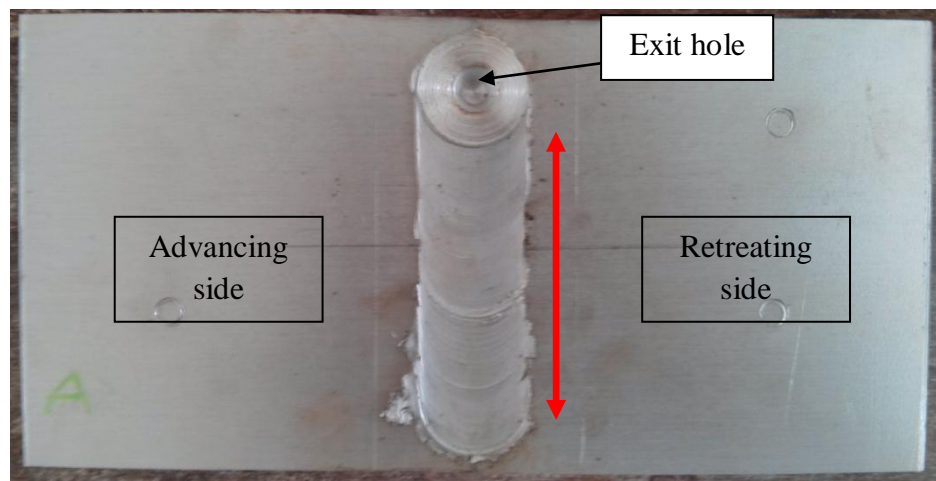


Figure 4. 1: FSW on Pass A

After the welded plate is sectioned by EDM machine, there is a presence of worm tunnel inside the welded plate as shown in figure below. The size of worm tunnel is about 1mm which can be considered as a very small defect. The worm tunnel is located along the red arrow as illustrated in the figure above. Normally, the

worm tunnel is associated with the porosity defect. Porosity is formed due to inadequate mixing and material flow between the pin and the aluminium alloy. There are many reasons that can cause inadequate mixing such as improper combination of pin rotational speed and also the traverse feed rate.



Figure 4. 2: Worm tunnel defect in Pass A.

4.1.2 Pass B (Double Passes on Same Side)

The second FSW is Pass B which consists of double passes welding. From the visual examination of Pass B welded plate, it can be observed that there is also no worm tunnel at the exit hole of Pass B. However, the worm tunnel defect inside the welded plate is still present but in a small size which is estimated around 1mm.

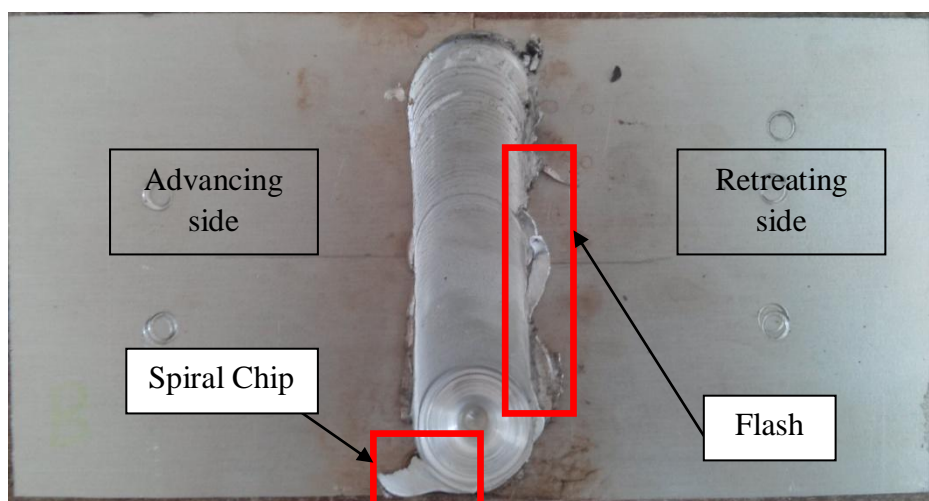


Figure 4. 3: The presence of spiral chip and flash on Pass B welded plate.

For Pass B, unlike Pass A, there is a presence of spiral chips near the exit hole. Heat generation mostly occurs at the surface contact between the tool shoulder

and the work piece. Significant heterogeneity in heat generation at that interface can lead to defect formation in the form of excess flash due to surface overheating [31].



Figure 4. 4: Presence of worm hole defects in Pass B

4.1.3 Pass C (Double Passes on Different Side)

Pass C is the last FSW process in this project which consists of double passes, one in the upper part and another one in the bottom part of the plate. It can be visually observe that Pass C does not have worm hole at the exit hole, the flash along

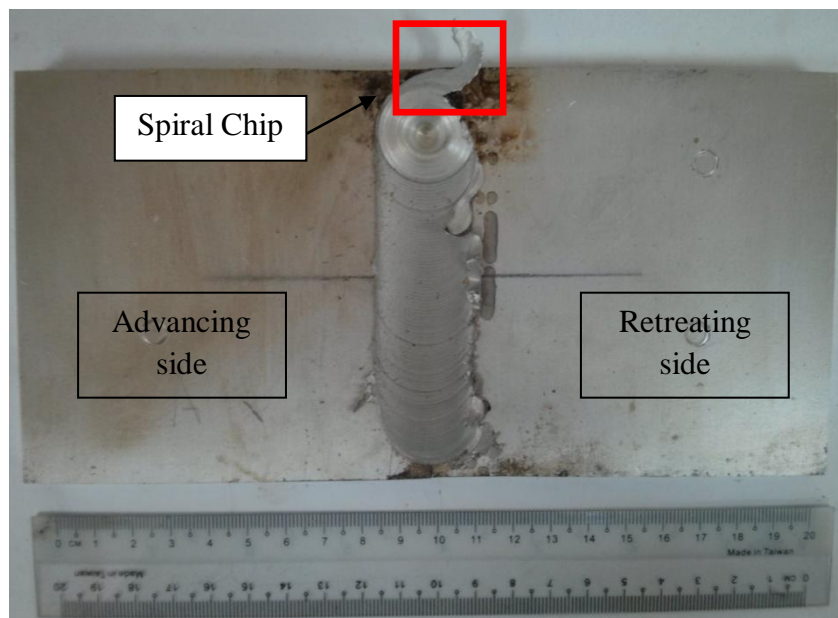


Figure 4. 5: Welded plate of Pass C

the welding line and also more spiral chip than Pass B. In addition, the worm hole defect inside of the welded plate is still presence. As can be observed from the picture, there is a dark area near the exit hole which indicate there has been the

highest heat generation during the welding. This is because for the second pass, the tool needs to overcome the increasing hardness that was caused from the first welding pass.



Figure 4. 6: Worm tunnel in Pass C welded plate.

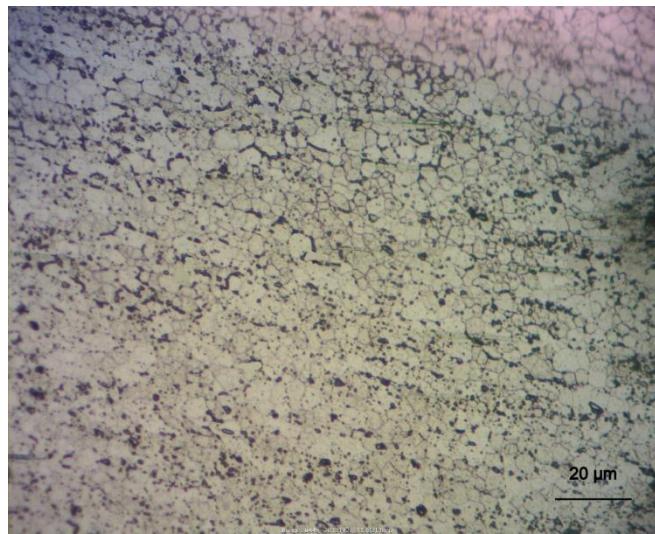
As can be seen from the figure of Pass A, B and C, all of the defects occur at the advancing side of the specimen. All of the tunnel defect can be seen by naked eye on the cross section area of welded region. Pass A exhibits the largest worm hole compare with Pass B and Pass C. This shows that the second pass of FSW in the Pass B and Pass C repair the defect that formed during the first pass. Therefore, only slight defect can be seen in Pass B and Pass C.

4.2 Microstructure Analysis

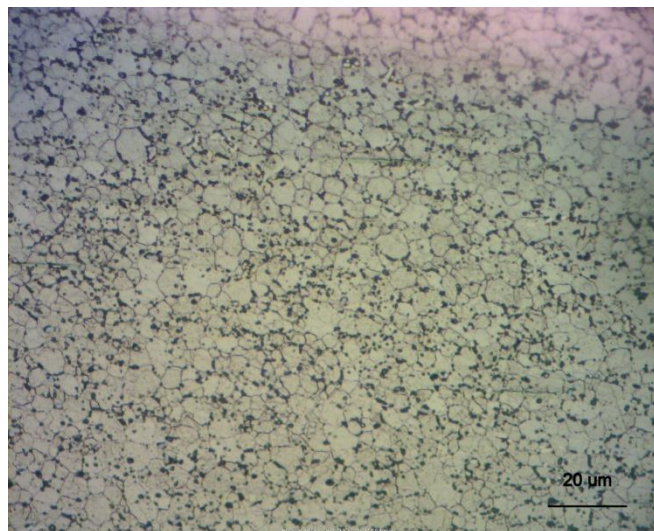
For microstructure analysis, there had been a lot of try and error process in order to get the clear visual of the grain boundary of three main zones which are stir zone, thermo-mechanically affected zone and heat affected zone. Figure below show the microstructure of Pass A, Pass B and Pass C.

Pass A (Single Pass)

a) SZ



b) TMAZ



c) HAZ

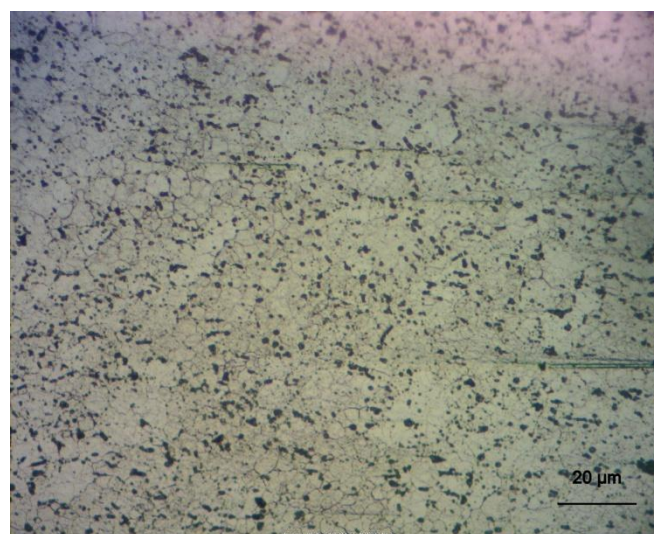
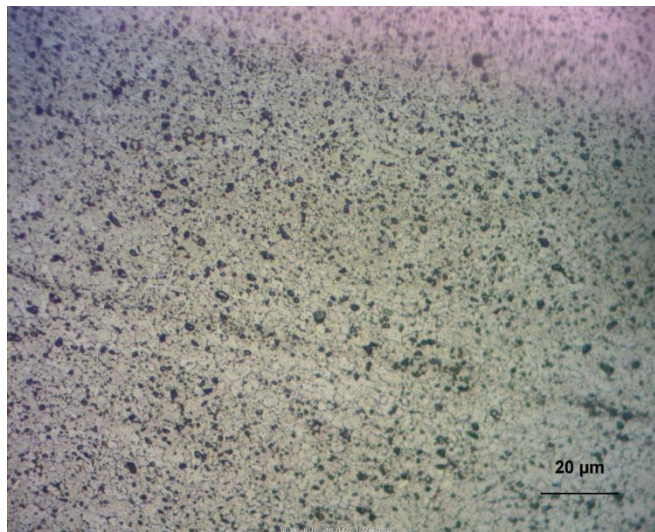


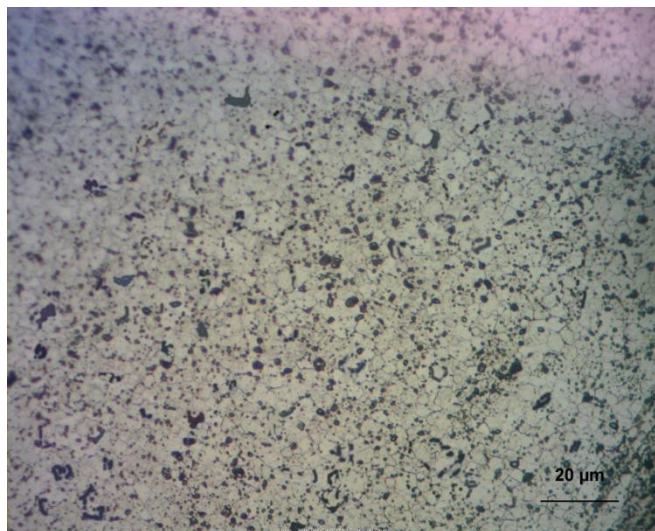
Figure 4. 7: Grain boundary microstructure 100x of three main regions of Pass A (Keller's etchant).

Pass B (Double Passes on Same Side)

a) SZ



b) TMAZ



c) HAZ

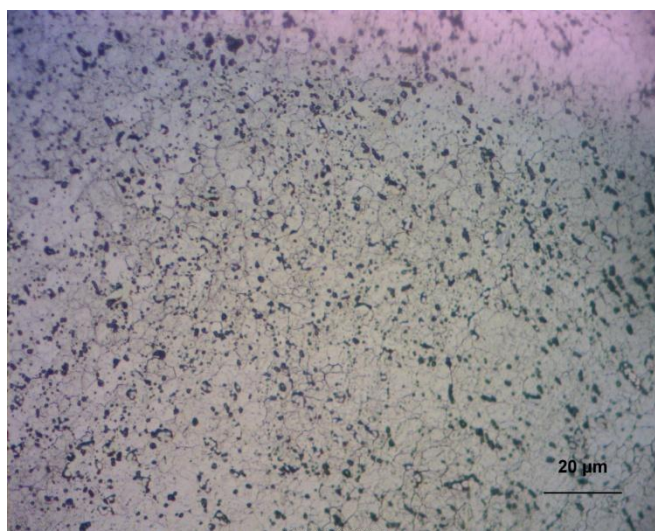
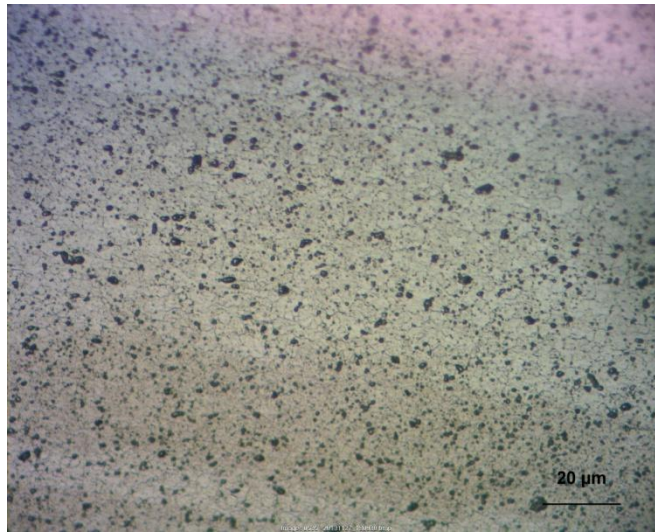


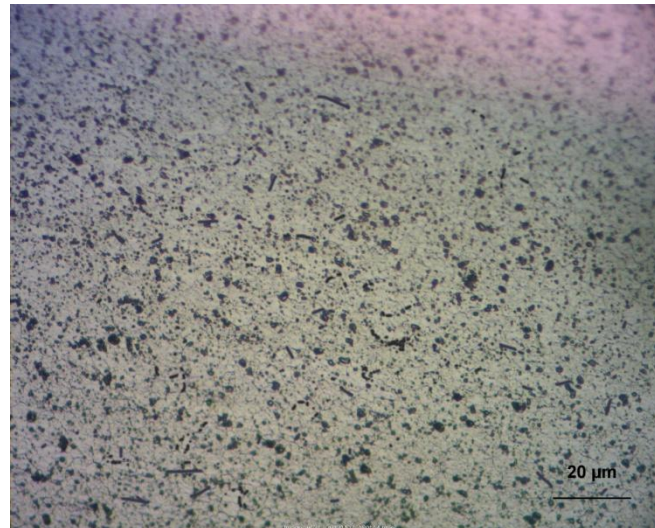
Figure 4. 8: Grain boundary microstructure 100x of three main regions of Pass B (Keller's etchant).

Pass C (Double Passes on Different Side)

a) SZ



b) TMAZ



c) HAZ

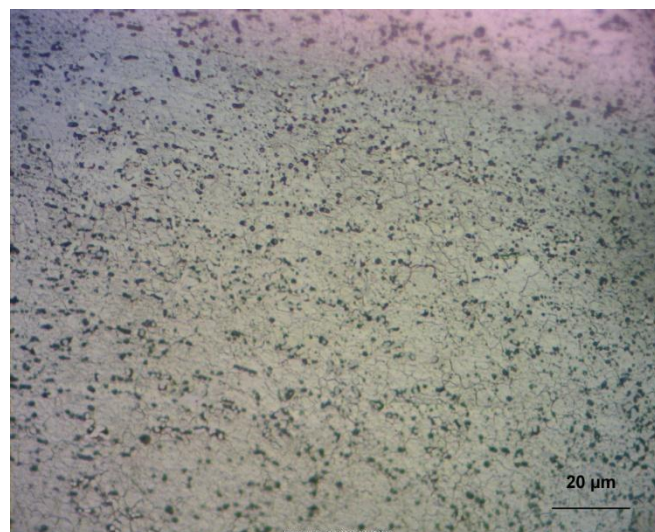


Figure 4. 9: Grain boundary microstructure 100x of three main regions of Pass C (Keller's etchant).

As can be observe from the above microstructure figure, the grain boundary in the stir zone (SZ) or weld nugget of Pass A, B and C consisted of dynamically recrystallized equiaxed grains. The size of the grain boundary ranges between 2.3 μm to 5.5 μm . However, Pass A which is the single pass FSW had the largest average grain boundary which is 3.7 μm to 5.5 μm compared with Pass B and Pass C that consist of two passes FSW. This result shows that the execution of more welding passes will produce smaller and finer grain. However, the grain size does not differ very much. Kwon et. al [32] in their research claimed that the grain recrystallization increases with the increasing welding temperature resulting from increasing tool rotation speed and this is proven in this project whereby same parameter was used in all welding passes and there was no much change in grain size. Besides, this also proved that no significant alteration in the mechanical properties occurs in this zone with the application of double welding passes [16].

In the thermo-mechanically affected zone (TMAZ), it can be observed that the grain size was slightly bigger than the weld nugget. The TMAZ region of aluminium alloy 6061-T6 displayed several numbers of precipitates which were more than SZ region and heat affected zone (HAZ) region. The precipitate occurred from the effect of the temperature distribution within and around the stirred zone ^[9]. FSW process can produced temperature around 400–550 °C within the weld nugget due to the friction between welding tool and workpieces as well as the plastic deformation around rotating pin[33] . As the welding temperature is very high, the precipitates in aluminum alloys can coarsen or dissolve into aluminum matrix depending on alloy type and also maximum temperature. TMAZ region undergo plastic deformation but the recrystallization did not occur in this region due to inadequate deformation strain ^[9].

In the heat affected zone (HAZ), the average grain boundary size for Pass A was 5.6 μm while for Pass B and Pass C was around 4.4 μm to 4.8 μm . The number of precipitates in HAZ remains high as seen in Figure 4.8 and Figure 4.9. In HAZ, the aluminium alloy experienced thermal cycle, but undergo only a little plastic deformation or none at all.

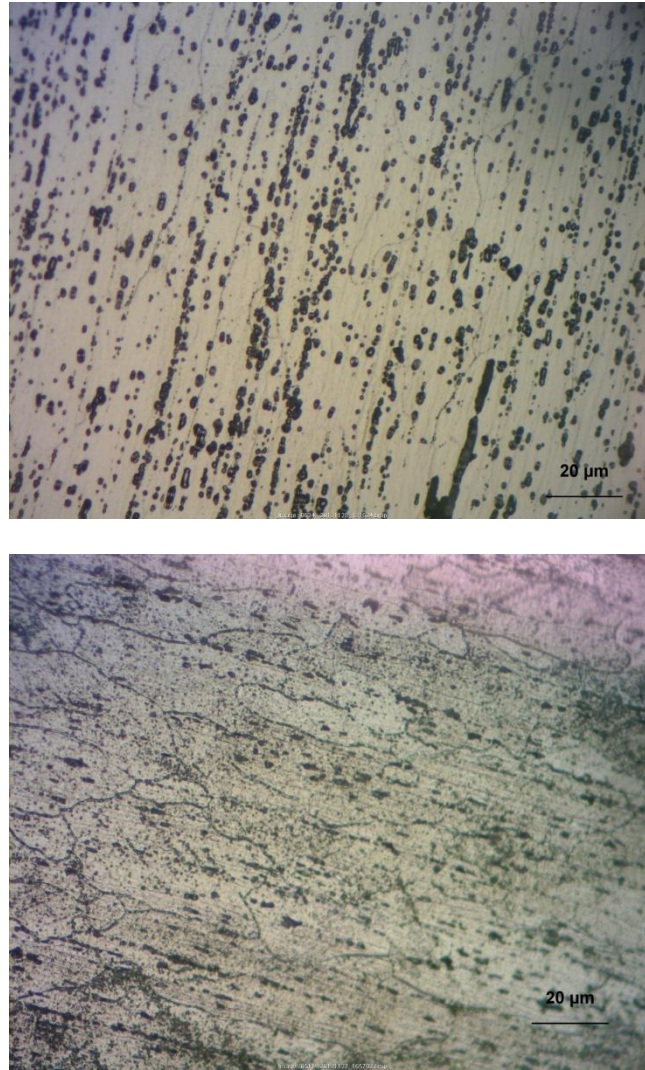


Figure 4. 10: Two different parent metal microstructure with 100x magnification (Keller's etchant)

From the figure above, it can be observed that the grain size of the parent metal (PM) was slightly elongated and larger than the other region. This observation is in agreement with the results of Mohammadtaheri *et. al* ^[21] and Li *et. al* [35] that also produced almost similar grain structure in their study. The elongated grain is believed resulted from the rolling process during the manufacturing of plate. The upper figure of parent metal showed a lot of precipitate while the lower figure showed a clear grain boundary of PM. This is because the interface between the recrystallized stir zone and the parent metal is relatively diffuse on the retreating side of the tool, but quite sharp on the advancing side [34].

4.3 Vickers Hardness Testing

Normally, researchers use hardness data as a preliminary evaluation of difference in mechanical properties across the weld zone. Hardness is resistance of material to plastic deformation caused by indentation. In FSW, micro-hardness profiles reflect the state of precipitates within the weld zone. As the alloy composition is already fixed, difference in micro-hardness must cause mainly from changes in precipitates and grain size. In this testing, a total of nine point of indentation were done in each pass to measure the HV value of welded plate. Figure below shows the schematic diagram of the indentation point of the welded plate.

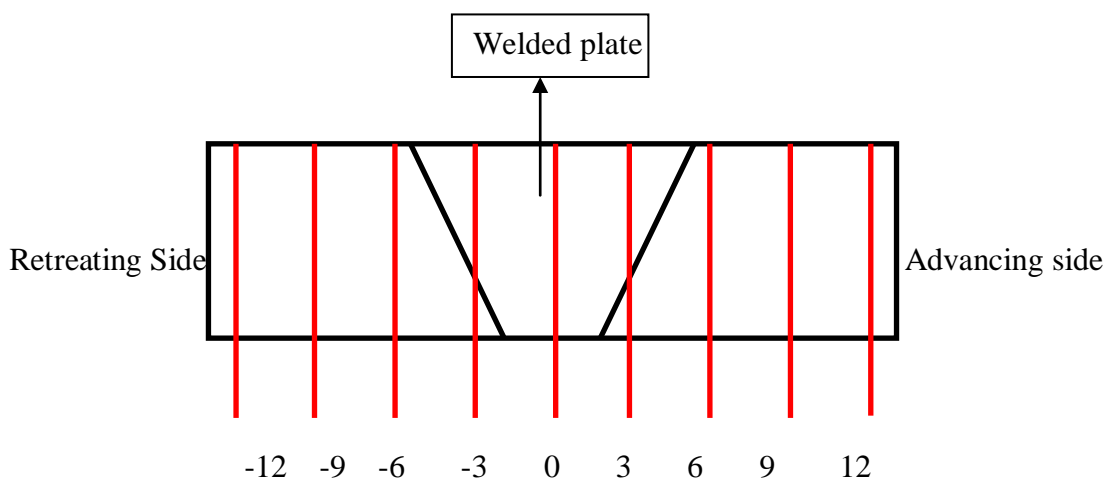


Figure 4. 11: Schematic diagram of Vicker's micro-hardness.

The spacing between each point is 3mm. Table below shows the value of HV of all nine points across the welded aluminium plate.

Table 4. 1: HV value of nine indentation hardness point

| Sample/Pass | -12 | -9 | -6 | -3 | 0 | 3 | 6 | 9 | 12 |
|-------------|------|------|------|------|------|------|------|------|------|
| | HV | HV | HV | HV | HV | HV | HV | HV | HV |
| A | 74.0 | 63.2 | 60.7 | 61.7 | 60.6 | 62.1 | 60.6 | 62.1 | 73.8 |
| B | 72.9 | 62.6 | 60.9 | 63.1 | 61.1 | 62.6 | 60.3 | 62.5 | 74.1 |
| C | 73.1 | 63.1 | 60.6 | 62.3 | 60.9 | 61.9 | 61.0 | 61.5 | 73.4 |

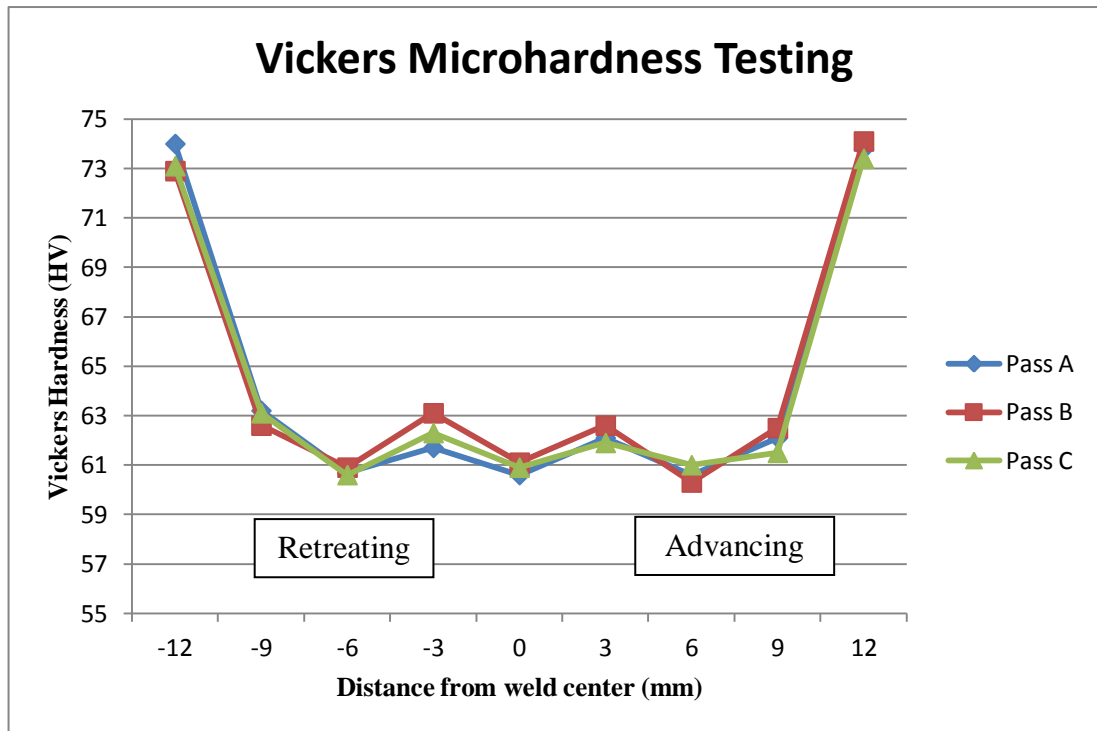


Figure 4. 12: Vickers hardness (HV) across the welded plate

As can be observed from the graph above, Pass A, Pass B and Pass C exhibit the typical W-shaped hardness profile across the welded plate. In the weld nugget, Pass B exhibits 61.1 HV which is the highest hardness value compared with Pass A and C. The hardness in the weld nugget of all passes is significantly lower than in the parent material. This is mainly due to the less number of precipitate that can result in the occurrence of dislocations in this region and reducing the hardness.

At the position of 3mm from the weld center which is the TMAZ region, all hardness value increase slightly whether in the advancing side or retreating side. Pass B exhibit the highest hardness in the TMAZ region with a value of 63.1 HV in the retreating side. The high hardness in the TMAZ region is result from the highest number of precipitate in this region. The precipitate impede the dislocation from occur. Thus, the hardness and strength increase in TMAZ.

In the HAZ region which is 6mm from the weld center, the hardness values decrease in all passes. The HAZ region exhibits the lowest hardness value compare with other region especially in the advancing side. This is mainly because of the

decreasing number of precipitate that located around the grain boundary in HAZ region. Besides that, the welding defect which is the worm hole that located around HAZ region also made the hardness value decreased.

It can be seen that the ultimate low point of hardness occur in between TMAZ and HAZ region. In TMAZ, Pass A exhibits the lowest hardness value while in HAZ, Pass B was the lowest among all passes. In overall, Pass B displayed the highest hardness average value, followed by Pass C and lastly Pass A. This shows that double passes exhibit higher hardness in single pass.

CHAPTER 5

CONCLUSIONS AND RECOMMENDATIONS

5.1 Conclusion

In conclusion, through the proper methodology from designing the welding tools to study microstructure investigation and micro-hardness testing, the project is understood to achieve its objective in studying the effect of different welding passes in Friction Stir Welding (FSW). It can be concluded that different welding passes will have effects on the welding result in FSW. From the welding visual examination, it can be observed that Pass A which consist of single pass exhibits bigger worm hole defects than Pass B and C which consist of double passes FSW.

From the microstructure investigation, several things can be concluded based on the result of the microstructure image that the author gets which are:

- ❖ The grain boundary in the weld nugget consists of dynamically recrystallized equiaxed grains.
- ❖ The average size of grain boundary in weld nugget of Pass A (single pass) is slightly bigger than Pass B and C (both double passes).
- ❖ Number of precipitates in TMAZ region is the highest compare with HAZ and SZ region
- ❖ Grain boundary of parent material in all passes is slightly elongated and larger than other region.

From the Vicker's micro-hardness testing, based on the nine indentation point using 1kg load, the things that can be concluded are:

- ❖ Hardness value in stir zone is lower than parent material.
- ❖ Pass B exhibits the highest hardness value in stir zone and TMAZ region.
- ❖ Hardness value in TMAZ region is higher than in the HAZ and stir zone region.

Thus, it can be concluded that among the three passes which are Pass A, Pass B and Pass C, the best passes with smallest average grain boundary size and highest hardness in the weld zone is Pass B which consists of double passes FSW on the same side of the aluminium plate.

5.2 Recommendations

Throughout the project which has been carried out for almost 9 months, there are several recommendations that can be done for future improvement such as:

- ❖ To have further study on effect of different welding passes especially for more than two passes. This can help to find a better finding and further improve the welding results in FSW.
- ❖ To have further study about different welding passes on dissimilar material such as aluminium and metal matrix composites (MMC).
- ❖ To provide a better polishing and grinding machine such as automatic polisher and grinder as this is the main part in producing a mirror-like sample and finding a good and clearer microstructure.

REFERENCES

- [1] W.M. Thomas, E.D. Nicholas, J.C. Needham, M.G. Murch, P. Templesmith, and C.J. Dawes: International Patent Application No. PCT/GB92/02203 and GB Patent Application No. 9125978.8, Dec.1991; U.S. Patent No. 5,460,317, Oct. 1995.
- [2] Z. Zhang and H.W. Zhang (2007) <www.sciencedirect.com> - Journal of Materials Processing Technology Numerical studies on controlling of process parameters in friction stir welding.mht
- [3] Mishra, R., Mahoney, M., and Lienert, T., "Friction Stir Welding and Processing V", 2009.
- [4] R. Brad and D. Lados. Microstructure-Property Correlations in Friction Stir Welded Al6061-T6 Alloys, 3-10.
- [5] J.A. Shneider and A.C. Nunes, Jr. (2003) Thermo-Mechanical Processing in Friction Stir Welds.
- [6] M. Mohammadtaheri, M. Haddad-Sabzevar, M. Mazinani and E.B. Motlagh (2013) The effect of base metal conditions on the final microstructure and hardness on 2024 aluminium alloy friction-stir welds, *Metallurgical and Materials Transactions B*, 44B, 738-743.
- [7] R.W. Fonda and J.F. Bingert (2004) Microstructural Evolution in the Heat-Affected Zone of a Friction Stir Weld, vol. 35A, 1487-1499
- [8] Friction Stir Welding. Retrieved 27 Jun 2013 from http://en.wikipedia.org/wiki/Friction_stir_welding
- [9] Mishra, R. S., & Ma, Z. Y. (2005). Friction stir welding and processing. *Materials Science and Engineering: R: Reports*, 50(1-2), 1-78.
- [10] Murr, L., Flores, R., Flores, O., McClure, J., Liu, G., and Brown, D. (1998)*Mate Res Innov* **1**.
- [11] Huijie, L., F(i, H., Maeda, M., and Nogi, K., (2003) Heterogeneity of mechanical properties of friction stir welded joints of 1050-H 24 aluminium alloy, *J Mater Sci Lett* **22**.
- [12] C.J. Dawes, (1999). Friction stir welding, *Talat Lecture 4410*, 1-13.

- [13] W.M. Thomas, I. M. Norris, D. G. Staines and E.R. Watts (2005) Friction Stir Welding – Process developments and variant techniques, *The SME Summit*, 1-21.
- [14] R. Rai , A. De, H. K D. H. Bhadeshia and T. Debroy (2011) Review : Friction stir welding tools, *Science and Technology of Welding ans Joining*, 16,325-342.
- [15] W.Y. Li, J.F. Li, Z.H Zhang, D.L Gao, and Y.J Chao (2013) Metal flow during friction stir welding of 7075-T651 aluminium alloy, *Experimental Mechanics*.
- [16] R.M Leal & A. Loureiro,(2007) Effect of Overlapping FSW Passes In the Quality of Welds of Aluminium Alloy , *Materials & Design* 29.982-991
- [17] Brown R.Tang.Wand Reynolds A.P (2009) Multi-pass friction stir welding in alloy 7050-T7451 : Effects on weld response variables and on weld properties, *Material Science and Engineering A*, 115-121.
- [18] T. Long, W. Tang, A.P. Reynolds, (2007)*Sci. Technol. Weld. Join.* 12 (4) 311–317.
- [19] K.A. Hassan, A.F. Norman, D.A. Price, P.B. Prangnell, (2003)*Acta Mater.* 51 1923–1936.
- [20] Xu. X. Yang. X.Zhou.G and Tong.J. (2012) Microstructure and fatigue properties of friction stir lap welds in aluminium alloy AA6061-T6, *Material and Design*, 175-183.
- [21] M. Mohammadtaheri, M. Haddad-Sabzevar, M. Mazinani and E.B. Motlagh (2013) The effect of base metal conditions on the final microstructure and hardness on 2024 aluminium alloy friction-stir welds, *Metallurgical and Materials Transactions B*, 44B, 738-743.
- [22] R.W. Fonda and J.F. Bingert (2004) Microstructural Evolution in the Heat-Affected Zone of a Friction Stir Weld, vol. 35A, 1487-1499
- [23] Frigaard, O., Grong, O., & Midling, O. T. (2001). A process model for friction stir welding of age hardening aluminum alloys. *Metallurgical and Materials Transactions A*, 32(5), 1189.
- [24] Reynolds, A., and Tang, W., (2001) “Alloy, Tool Geometry, and Process Parameter Effect on Friction Stir Welding Processes”, *Friction Stir Welding and Processing*, Jata, K., Mahoney, M., Mishra, R., Semiatin, S., and Field, D., Ed., TMS.

- [25] R. Rai , A. De, H. K D. H. Bhadeshia and T. Debroy (2011) Review : Friction stir welding tools, *Science and Technology of Welding ans Joining*, 16,325-342.
- [26] S. Koizumi, M. Tsujikawa, T. Oguri, & K. Higashi (2007) Two pass fsw joint of magnesium alloy, *Advanced Material Research*,15-17, 363-368.
- [27] R. Armagan, & S. Tamer (2005) Effects of double passes of the tool on friction stir welding of polyethylene, *Journal of Material Science*, 40, 3313-3316.
- [28] W. A. Christian, F. John, J.K Barat, & W. K. Micheal (2013) Mechanical properties of repaired 7075-T73 friction stir weld butt welds, *Friction Stir Wldeing and Processing VII* ,205-212.
- [29] S. Natalia (2012) On the machinability of high performance tool steels, 16-18.
- [30] Vickers Hardness Test. Retrieved 20 September 2013 from <http://www.gordonengland.co.uk/hardness/vickers.htm>
- [31] Kim, Y., Fuji, H., Komazaki, T., Nakata, K., “Three defect types in friction stir welding of aluminum die casting alloy” (2005)
- [32] Kwon YJ, Saito N, Shigematsu I. (2002) Friction stir process as a new manufacturing technique of ultrafine grained aluminium alloy, *J Mater Sci Lett*, 21:1473-6.
- [33] C.G. Rhodes, M.W. Mahoney, W.H. Bingel, R.A. Spurling, C.C. Bampton (1997) *Scripta Mater.* 36 ,69.
- [34] M. James, M. Mahoney, in: *Proceedings of the First International Symposium on Friction Stir Welding*, Thousand Oaks, CA, USA, June 14–16, 1999.
- [35] Li, Y., Murr, L.E. & McClure, J.C. (1999). Flow visualization and residual microstructures associated with the friction-stir welding of 2024 aluminum to 6061 aluminum. *Materials Science and Engineering A*, Vol. 271, pp. 213-223.

APPENDIX

Appendix A

